NASA TECHNICAL MEMORANDUM

NASA TM X-67817

EFFECT OF RADIOMETRIC ERRORS ON ACCURACY OF TEMPERATURE-PROFILE MEASUREMENT BY THE SPECTRAL-SCANNING METHOD

by D. R. Buchele
Lewis Research Center
Cleveland, Ohio

Effect of Radiometric Errors on Accuracy of Temperature-Profile Measurement by the Spectral-Scanning Method

D. R. Buchele

NASA Lewis Research Center, Cleveland, Ohio 44135

Abstract

The spectral-scanning method may be used to determine the temperature profile of a jet- or rocket-engine exhaust stream by measurements of gas radiation and transmittance, at two or more wavelengths. A single, fixed line of sight is used, using immobile radiators and radiometers outside of the gas stream, and there is no interference with the flow. A given radiometric error causes an error in computed temperatures. The ratio between temperature error and radiometric error depends on profile shape, path length, temperature level, the strength of line absorption, and the absorption coefficient and its temperature coefficient. These influence the choice of wavelengths, for any given gas. Conditions for minimum temperature error are derived. Numerical results are presented for a two-wavelength measurement on a family of profiles that may be expected in a practical case of H_2 - O_2 combustion. Under favorable conditions, the fractional error in temperature approximates the fractional error in radiant-flux measurement. For small path lengths, where gas absorptance is small, the temperature error may be minimized by choosing widely-separated wavelengths.

nondimensional quantities, such as temperature ratios or distance ratios, that define the shape of the temperature-distribution curve.

Each of the "independent measurements" mentioned actually consists of the usual set of three flux measurements used in absorption-emission pyrometry: flux from the gas alone, flux from a reference source alone, and flux from the reference source after it has passed through the gas.

The accuracy with which one can determine the temperature distribution will depend on the judicious choice of the weighting functions for the individual integrals. Thus, the choice of the spectral interval which each measurement favors must be such as to maximize the accuracy of temperature measurement This paper addresses itself to the problem of spectral-interval selection, for the case $j = 2$, for profiles that might be encountered in turbojet, ramjet, or rocket engines using hydrogen as the principal fuel and oxygen as the principal oxidant.

The problem definition also requires an exact definition of what is meant by "accuracy." The measure of accuracy that will be used in this report will be the error in temperature at one selected location along the path.

The temperature distribution will be assumed to be represented by a curve characterized by two parameters - a temperature and a numeric that defines the shape of the curve. The fractional error in temperature due to a given fractional error in flux measurement will then be computed for various combinations of wavelength and absorp-

tion coefficient, in order to identify the combination that yields the smallest fractional error in temperature. In order to provide specific numerical results, the example of infrared radiation from H_2O, as developed in $H_2 - O_2$ or H_2-air combustion, will be treated in some detail.

SYMBOLS

A	spectrometer constant
b	average line spacing
c_2	second radiation constant
D	derivative, Eq. (18)
E	error ratio
f, F	factors in error formulas
g, G	slit functions
H	temperature coefficient of absorption coefficient
k	absorption coefficient
L	path length
m	number of zones
N_λ	spectral radiance
n	profile shape parameter
P	pressure
T	temperature
u	optical depth
v, V	factors in error formulas
x	distance along path
y	function of x/L

β fine-structure coefficient

γ line half-width

ϵ absorption coefficient error ratio

η exponent

λ wavelength

$\Delta\lambda$ effective slit width

$\sigma_1 - \sigma_4$ summations

τ transmission factor

φ flux

Subscripts

0   reference

a, b   set of measurements

av   average

L   value at $x = L$

ANALYSIS

Method of Treatment

In absorption-emission pyrometry, three flux measurements φ_1, φ_2, and φ_3 are made. These represent, respectively, the fluxes from the gas column alone, from the source alone, and from the source after passing through the gas column. It is convenient for computational purposes also to introduce an intermediate variable, the overall transmission factor $\tau_L = \varphi_3/\varphi_2$.

In the spectral-scanning method, several sets of such measurements are made, at different wavelengths and perhaps at different effective slit widths. The number of sets must be not less than the number of independ-

ent parameters that characterize the temperature distribution along the gas column. When the number of sets exceeds the number of parameters, the redundancy helps to reduce the statistical inaccuracy of the results. In this paper, the temperature distribution over the path $0 \le x \le L$ will be assumed to be characterized by two parameters: a temperature T_m and a nondimensional factor n that characterizes the shape of the temperature profile. Thus,

$$T = T(x, T_m, n) \tag{1}$$

It will be assumed that two sets of flux measurements are made, assigned subscripts a and b, respectively, and that, for each set, one may select a mean wavelength λ and a slit width $\Delta\lambda$. The formal error analysis problem is to determine the error in the deduced values of T_m and n due to errors in the six flux measurements. The inverse experiment-design problem is to determine values of λ_a, λ_b, $\Delta\lambda_a$, and $\Delta\lambda_b$ that will lead to low values of the errors $|\delta T_m/T_m|$ and $|\delta n/n|$ when all six flux measurements have the same fractional error $|\delta\varphi/\varphi|$. The solution of the problem requires assumption of a physical model of the mechanisms of spectral emission and absorption at each of the two spectrometer settings. Specifically, in the present treatment, it requires assumptions of the magnitude and temperature coefficient of the absorption coefficient.

A convenient approach to the problem is to compute the fluxes for an assumed temperature distribution so that the φ_a's and φ_b's are expressed as functions of T_m and n. Differentiation then relates the error in each φ to errors in T_m and n through formulas of the general form

$$d\varphi = (\partial\varphi/\partial T_m)dT_m + (\partial\varphi/\partial n)dn \qquad (2)$$

Solution of the simultaneous relations then yields the inverse expression of dT_m and dn in terms of the errors in the individual φ's. The algebraic expressions are then converted to a statistical summation of errors by summing the squares of the individual, independent error terms. Finally, the individual values of fractional error in flux measurements are set equal to each other to establish the error ratios

$$E(T_m) \equiv \left| (\delta T_m/T_m)/(\delta\varphi/\varphi) \right|$$
$$E(n) \equiv \left| (\delta n/n)/(\delta\varphi/\varphi) \right| \qquad (3)$$

General Equation for Gas Radiation

The flux from a nonisothermal gas column of length L, measured by a receiver located at $x = 0$, is

$$\varphi_1 = A \int_0^\infty g(\lambda) \int_0^L N_\lambda(\lambda, x)k(\lambda, x)\exp\left[-\int_0^x k(\lambda, \xi)d\xi \right]dx\, d\lambda \qquad (4)$$

where A is a constant of the spectrometer, equal to the product of spectrometer transmission factor, entrance-slit area, and dispersing-element area (or collimating-element area if there is one between the slit and the dispersor), divided by the square of the distance between slit and dispersor.

The spectral radiance N_λ is given adequately for error analysis by Wien's approximation to Planck's equation. The exponential is the gas transmission factor $\tau(\lambda, x)$. Plass[2] shows that the product $k(\lambda, x)\tau(\lambda, x)$ may be written as $\partial\tau(\lambda, x)/\partial x$.

The spectrometer slit function $g(\lambda)$ is appreciably different from zero over only a narrow span of wavelength. We define the effective

8

slit width $\Delta\lambda$ as representing this span, and represent the integral by G, so that

$$G \equiv \int_0^\infty g(\lambda)d\lambda = \int_{\Delta\lambda} g(\lambda)d\lambda \tag{5}$$

Equation (4) may be integrated over the wavelength by use of two approximations: (1) when $\Delta\lambda$ is small, N_λ may be considered independent of λ over the span $\Delta\lambda$; (2) when a spectral band model is available that allows one to effectively integrate $\tau(\lambda, x)$ over the span $\Delta\lambda$, τ may be considered independent of λ over this span and $\tau(\lambda, x)$ may be replaced by

$$\tau(x) = \int_{\Delta\lambda} g(\lambda)\tau(\lambda, x)d\lambda \Big/ \int_{\Delta\lambda} g(\lambda)d\lambda \tag{6}$$

If the band model is to be valid, $\Delta\lambda$ must include enough spectral lines to produce an average τ that is not sensitive to a further increase in $\Delta\lambda$. On the other hand, $\Delta\lambda$ must be small enough so that it lies within the band and so that it does not exceed the limits within which conditions (1) and (2) are reasonably valid.

With the approximations indicated above, Eq. (4) becomes

$$\varphi_1 = AG \int_0^L N_\lambda(x) \cdot \left[d\tau(x)/dx\right]dx \tag{7}$$

In the absorption-emission method, where measurements are made of φ_1 and of $\tau(L) = \varphi_3/\varphi_2 \equiv \tau_L$, all three fluxes must be measured with the same value of G.

Equation (7) cannot be integrated analytically with most temperature profiles found in practice, but adequate numerical integration can be performed with any smooth profile. The path is divided into m isothermal zones, so that Eq. (7) becomes

$$\varphi_1 = A\,G \sum_{i=1}^{m} \overline{N}_i (\tau_i - \tau_{i+1}) \tag{8}$$

where $\overline{N}_i$ is the arithmetic average of $N_{\lambda,i}$ and $N_{\lambda,i+1}$ and τ_i is computed, using a band model, as described in the next section.

Gas Transmission Function

The band-model formulation for a nonisothermal gas is based on Eq. (5) of Ref. 3. This formulation has been justified and applied in Ref. 4, and summarized in Ref. 5. The transmission factor τ is a function of optical depth u given by

$$\tau = \exp\left\{-u\Big/\left[1 + (\pi u/2\beta_{av})\right]^{1/2}\right\} \tag{9}$$

$$u = \int_0^x k(\beta/\beta_{av})^\eta \, dx \tag{10}$$

$$\beta_{av} = \left[\int_0^L (\beta P/T)dx\right]\Big/\int_0^L (P/T)dx \tag{11}$$

where k is the absorption coefficient at temperature T and partial pressure P, and β is the fine-structure coefficient. Both k and β are functions of T and hence of location x along the optical path $0 \le x \le L$. The value of β may be computed as

$$\beta = 2\pi\gamma/b \tag{12}$$

where γ is the line half-width and b is average line spacing. The quantities k, γ, and b must be known. The quantity β_{av} is a mass-weighted average of β over the entire path. An empirically-derived specification of the exponent η in terms of the overall optical depth u_L is

$$\eta = 0 \text{ for } u_L = 1; \ \eta = 1 \text{ for } u_L = 10;$$
$$\eta = (u_L - 1)/9 \text{ for } 1 \le u_L \le 10. \tag{13}$$

Although the above equations are used directly for profile determination, approximations are necessary to permit presentation of the results of an error analysis in sufficiently simple form. It is impractical to treat both k and β as independent parameters; the number of independent parameters must be limited to those with the greatest effect on accuracy. The variables we choose are the overall transmission factor $\tau(L) \equiv \tau_L$, the temperature coefficient H of the absorption coefficient, and the wavelength λ. The wavelength is important because of its strong influence on the spectral radiance, through Planck's law. The transmission factor is chosen in preference to the absorption coefficient because the former includes the effect of path length. A convenient and adequate approximation of H is computed by using the linearization

$$k_0(T) = k_0(T_m)(T_m/T)\left[1 + H(T - T_m)/T_m\right] \tag{14}$$

where k_0 is the absorption coefficient at standard reference pressure P_0, and taking $T = T_m - 2(T_m - T_{av})$, where T_{av} is a temperature that is representative of the major flux-contributing portion of the path. When Eq. (14) leads to a negative value of $k_0(T)$, $k_0(T)$ is to be taken as zero. A reasonable criterion for choosing T_{av} is

$$T_{av} \approx (1/L) \int_0^L T(x)dx \tag{15}$$

To calculate $\tau(x)$, the following procedure is therefore followed:

Given $T(x)$ from the assumed temperature profile, $P(T)$ from the gas composition and partial pressure, and β from a direct tabulation or from values of γ and b, find β_{av} by Eq. (11). From the measured $\tau_L \equiv \tau(L)$, solve Eq. (9) for u_L and then estimate η from Eq. (13). Assuming a value of H, Eqs. (12) and (14) are used to express $k_0(T)$ in terms of $k_0(T_m)$ in Eq. (10). Integrating Eq. (10) over the entire path length L then yields

$$k_0(T_m) = u_L P_0 \Big/ T_m \int_0^L (P/T)\big[1 + H(T - T_m)/T_m\big](\beta/\beta_{av})^\eta \, dx \tag{16}$$

With $k_0(T_m)$ known, Eqs. (14), (12), (10), and (9) are now used, in that order, to determine $\tau(x)$.

Error Analysis

Error analysis is effected by differentiation of Eq. (8) and then replacing differentials of significant quantities by the errors in those quantities. Differentiation of Eq. (8) requires determination of the differentials $d\overline{N}_i$ and $d(\tau_i - \tau_{i+1})$. The expression for $d\overline{N}_i$, obtained by differentiating Wien's equation, is

$$d \overline{N}_i = \big[c_2 \overline{N}_i/(\lambda T_i^2)\big] dT_i \tag{17}$$

where dT_i is represented in terms of T_m and n through the differential of Eq. (1), and c_2 is Planck's second radiation constant.

The differential $d(\tau_i - \tau_{i+1})$ is evaluated numerically as follows: the value of $\tau_i \equiv \tau(x_i)$ having been determined for given H, T_m, n, and τ_L, an increment $d\tau_L$ is introduced, keeping H, T_m, and n constant, and a new value of τ_i is calculated. The difference is then $d\tau_i$. This procedure is repeated for τ_{i+1} to establish $d\tau_{i+1}$. The derivative

$$D_i = (d\tau_i - d\tau_{i+1})/d\tau_L \tag{18}$$

is then computed. We note in passing that

$$d\tau_L/\tau_L = (d\varphi_3/\varphi_3) - (d\varphi_2/\varphi_2) \tag{19}$$

but continue to work with τ_L for conciseness.

When Eq. (8) and its differential are combined with Eqs. (17) and (18) and the differential of Eq. (1), the result may be written as

$$\frac{dT_m}{T_m} - f\, dn = V \equiv v_1 \frac{d\varphi_1}{\varphi_1} - v_2\, d\tau_L \tag{20}$$

where f, v_1, and v_2 depend on the temperature profile.

When two sets of measurements are made, identified by respective subscripts a and b there result two equations of the form of Eq. (20) representing the differentials in the six flux measurements (through Eq. (19)) due to differentials dT_m and dn. Simultaneous solution of the two equations yields

$$dT_m/T_m = (f_a V_b - f_b V_a)/(f_a - f_b) \tag{21a}$$

$$dn = (V_b - V_a)/(f_a - f_b) \tag{21b}$$

If all six flux measurements are now assigned equal fractional error, the corresponding errors in T_m and n are given by

$$E^2(T_m) = (f_a^2 F_b^2 + f_b^2 F_a^2)/(f_a - f_b)^2 \tag{22}$$

$$E^2(n) = (1/n^2)(F_b^2 + F_a^2)/(f_a - f_b)^2 \tag{23}$$

where

$$F^2 = v_1^2 + 2v_2^2 \tau_L^2 \tag{24}$$

with subscript a or b assigned to F, τ_L, f, v_1, v_2, and the error ratios are defined by Eq. (3). These represent the sensitivity of T_m and n to errors in flux measurement. The sensitivity is greatest when $f_a \approx f_b$; hence this difference should be held large, while the F-values should be as small as possible.

Alternative determination of absorption. - In those situations when τ_L is near unity, so that F becomes large, a smaller value of F may be obtained by estimating τ_L by analytic computation rather than from experimental flux measurements φ_2 and φ_3. This alternative approach is possible if a tabulation of k_0 is available and if a good a priori estimate of the temperature profile can be made. (This estimate might be the profile first determined by the three experimental flux measurements.) Let $\epsilon = (dk_0/k_0)/(d\varphi/\varphi)$ be the ratio of the error of the tabulated k_0 to the error of flux measurement. Then Eq. (24) can be replaced by

$$F^2 = v_1^2 + v_2^2 \tau_L^2 (\epsilon \ln \tau_L)^2 \tag{25}$$

Accuracy is thereby improved whenever $(\epsilon \ln \tau_L)^2 < 2$.

EXAMPLE

Assumptions and Data for Computation of f and F

To clarify what magnitudes of error ratios might be achieved in a practical application and what control might be exercised on these error

ratios, numerical calculations have been made for a specific family of temperature profiles and for the infrared radiation from H_2O.

The profiles will be assumed to be given by

$$(T_m - T)/(T_m - T_L) = y^{1/n} \tag{26}$$

where

$$y = |(2x/L) - 1| \tag{27}$$

and

$$T_L = 300K, \qquad 1000 \leq T_m \leq 3000K, \qquad 0 < n \leq 1/2$$

These profiles are shown in Fig. 1. They resemble the transverse velocity and temperature distributions often found in ducts with axisymmetric flow.

For this profile, dT_i in Eq. (17) becomes

$$dT_i = (1 - y_i^{1/n})dT_m$$

$$+ (T_m - T_L)(y_i^{1/n} \ln y_i)(1/n^2)dn \tag{28}$$

and the values of f, v_1, v_2 in Eq. (20) become

$$f = \sigma_2 (T_m - T_L)/(\sigma_1 T_m n^2)$$

$$v_1 = \sigma_3 (T_m - T_L)\lambda/(\sigma_1 c_2 T_m)$$

$$v_2 = \sigma_4 (T_m - T_L)\lambda/(\sigma_1 c_2 T_m)$$

$$\sigma_1 = \sum \bar{N}_i (\tau_i - \tau_{i+1})(\bar{T}_i - T_L)/\bar{T}_i^2$$

$$\sigma_2 = \sum \bar{N}_i (\tau_i - \tau_{i+1})(\ln y_i)(\bar{T}_i - T_m)/\bar{T}_i^2$$

$$\sigma_3 = \sum \bar{N}_i (\tau_i - \tau_{i+1}) = \varphi_1/AG$$

$$\sigma_4 = \sum \bar{N}_i D_i$$

$$\bar{T}_i = (T_i + T_{i+1})/2$$

(29)

where all summations are for $i = 1$ to $i = m$.

The values of F in Eqs. (24) and (25) are adequately approximated by

$$F/(\lambda T_m) \approx 0.62 \left\{ 1 + 2\left[{}^m\tau_L/(1 - {}^m\tau_L)\right]^2 \right\}^{1/2} \tag{30}$$

$$F/(\lambda T_m) \approx 0.62 \left\{ 1 + \left[\epsilon\, {}^c\tau_L \ln {}^c\tau_L/(1 - {}^c\tau_L)\right]^2 \right\}^{1/2} \tag{31}$$

where ${}^m\tau_L$ is the ratio of the measured fluxes φ_2 and φ_3, while ${}^c\tau_L$ is calculated from a tabulation of absorption coefficient. Equations (30) and (31) are plotted in Fig. 2.

The H_2O radiation will be assumed to lie within the 1.9, 2.7, and 6.3μm bands. Other assumed limits will be

overall transmission factor $0.1 < \tau_L < 1$

temperature coefficient of k $-3 \le H \le 2$

For the profiles of Eq. (26), Eq. (15) leads to values of T_{av} that lie between 70 and 100 percent of T_m. Therefore a safe rule of thumb for

T_{av} is $T_{av} \approx 0.85 T_m$. Table I gives values of k_0 and H for wavelengths that are of particular interest, because their use can lead to relatively small values of the error ratios. The values in Table I are computed from the tabulations by Ludwig, et al[6] of values of $k_0 T_m/T_0$ at 1 atm. pressure. The value of ϵ for the data is on the order of 10.

The values of γ and b are also computed from Ref. 6. Using values there tabulated, one obtains

$$\gamma = 0.09(1/P_0)(T_0/T)^{1/2}\left(P_{H_2O} + P_{N_2}\right) + 0.44(T_0/T)\left(P_{H_2O}/P_0\right) \quad (32)$$

The value of b (designated d in Ref. 6) can be approximated for H_2O by making it independent of wavelength and with a temperature dependence given by

$$b = b_0(T_0/T)^3 \quad (33)$$

where

$$b_0 = 0.5 \quad \text{at} \quad T_0 = 1500 \text{ K}$$

For a given amount of fuel and oxidant, the more important partial pressures P_{H_2O} and P_{N_2} can be determined[7] to allow computation of γ. The approximations make $\beta(T)$ the same at all wavelengths in the range of λ.

The error-ratio parameter f, Eq. (29), is plotted in Fig. 3 for a particular wavelength in each of three H_2O bands for $\tau_L = 0.6$; interpolation may be used for any other wavelength. The quantity f is affected to a lesser degree by τ_L than it is by λ or H (f increases as τ_L decreases). On the other hand, parameter F, Eqs. (30) and (31), is more strongly affected by τ_L than it is by λ or H.

To find a value of F by use of Fig. 2b, $\bar{\tau}$ must be estimated from the optical depth kL. Figure 4 shows the relation between τ_L and the optical depth kL of an isothermal gas column, in accordance with Eq. (9). The optical depth of a nonisothermal gas column is an integral of the local value of k over the path L. For the profile of Eq. (26), this integral is approximated by

$$kL = k_0(T_m)(LP/P_0)\left[1 + 2n(1 - H)(T_m - T_L)^2/T_m^2\right] \qquad (34)$$

for $H \leq T_m/(T_m - T_L)$. Since a larger value of H would give a negative value of k at T_L, the quantity H should arbitrarily be assigned the limiting value $T_m/(T_m - T_L)$ if H is actually larger than this value. Pressure P of the emitting gas is a representative value over the temperature range from T_L to T_m. Representative values of P and β are their values at the temperature T_{av} used in the determination of H.

Procedure for Computing Error Ratios

The steps in the computation of error ratios are:

1. For given T_m, n, H, and λ, obtain the values of f from Fig. 3.

2. For given L, and partial pressure P, use Eq. (34) and Table I to compute the optical depth.

3. Compute, at temperature $T_{av} = 0.85\,T_m$, γ from Eq. (32), and b from Eq. (33), assuming $b_0 = 0.5$.

4. Calculate β from Eq. (12).

5. Obtain τ_L from Fig. 4.

6. Obtain F from Fig. 2, choosing the procedure (measurement or calculation) which yields the smaller value.

7. Calculate the error ratios by Eqs. (22) and (23).

Computed Error Ratios

The error ratios are plotted in Fig. 5 against path length L for three cases: both measurements in the same band (2.7μm); measurements in adjacent bands (2.7μm, 6.3μm); measurements in widely-different bands (1.9μm, 6.3μm). The decrease of error ratio as L increases is due to the corresponding reduction in τ_L and F, since parameter f remains constant. Values of $^m\tau_L$ and $^c\tau_L$ along the curves are listed in Table II. The error ratio is smaller at lower temperatures because (1) F is proportional to T_m, (2) F decreases with decreasing τ_L, which decreases with decreasing temperature, unless path length also decreases. For example, at a path length of 10 cm the lowest obtainable error ratio $E(T_m)$ is about 7 at 3000 K and about 2 at 1000 K.

PROCEDURE FOR SELECTING OPTIMUM WAVELENGTHS

Given a gas of path length L, pressures $P_{H_2O} \equiv P$ and P_{N_2}, wall temperature T_L, and prior estimates of T_m and n, the following steps may be used to select the pair of wavelengths λ_a, λ_b that will minimize the error ratios $E(T_m)$ and $E(n)$.

1. Use Fig. 3 to select approximate values of λ_a, λ_b and corresponding parameters H to minimize the error ratio in accordance with the selection rule to keep $|f_a - f_b|$ large, and in accordance with considerations of convenience such as availability of detectors, fitters, or monochromators. Use step (2) to confirm that the chosen combination of H and λ exists.

2. By use of Table I, choose wavelengths λ_a, λ_b, at which the desired values of H occur. The error ratio is minimized when the longer wavelength has the more negative value of H, and the larger value of k.

3. Compute error ratios by the steps listed under "Procedure for Computing Error Ratios."

CONCLUDING REMARKS

The preceding discussion has treated errors resulting from uncertainty in flux measurement. Additional sources of error lie in the knowledge of the characteristics of the gas itself; these include the validity of the band model and, through it, the accuracy of the band-model parameters k and β. These are affected also by uncertainties in knowledge of gas composition. On the other hand, the two wavelengths and the corresponding Planck function are known with negligible error. The use of widely separated wavelengths generally results in a desirably larger value of the quantity $|f_a - f_b|$. Such a large value of the difference is less dependent on the value of H or τ_L or on uncertainty in the band model computation of $\tau(x)$ by Eq. (9).

The examples show that $E(T_m)$ increases as T_m increases and is quite large at short path lengths. The resultant error ratio may be excessive. It is therefore appropriate to consider more desirable alternatives. One such alternative is to dispense with the restriction to infrared radiation and to examine the possible advantages of using ultraviolet radiation as well as infrared. At temperatures above 2000 K the pressure of OH is sufficient to permit the measurement of its radiation in the ultraviolet. It is then possible to make one temperature measurement with OH radiation, and only one temperature measurement with H_2O radiation. The

wavelength separation between ultraviolet and infrared is large. This wavelength separation results in a large difference of parameters $\left| f_a - f_b \right|$. The short wavelength of OH reduces the value of F, which is proportional to λT_m, and of f to a lesser degree, as indicated by Fig. 3.

If the method of temperature measurement with OH were not of the absorption-emission type, the quantitative conclusions of the present analysis would not hold, but the method of approach would still be valid.

REFERENCES

1. R. H. Tourin: Spectroscopic Gas Temperature Measurement (Elsevier Pub. Co., New York, 1966).

2. G. N. Plass: "Radiation from Nonisothermal Gases," Appl. Opt. 6, 1995 (1967)

3. F. S. Simmons: "Band Models for Nonisothermal Radiating Gases," Appl. Opt. 5, 1801 (1966).

4. F. S. Simmons; H. Y. Yamada; and C. B. Arnold: "Measurement of Temperature Profiles in Hot Gases by Emission-Absorption Spectroscopy," Michigan University Report WRL-8962-18-F, NASA CR-72491 (1969).

5. F. S. Simmons; C. B. Arnold; G. H. Lindquist; and F. G. Smith: "Calculation of Radiation from Hot H_2O and CO_2 Viewed Through a Cool Intervening Atmosphere," Appl. Opt. 9, 2792 (1970).

6. C. B. Ludwig: "Study on Exhaust Plume Radiation Prediction," General Dynamics/Convair, NASA CR-61233 (1968).

7. F. J. Zeleznik; and S. Gordon: "A General IBM 704 or 7090 Computer Program for Computation of Chemical Equilibrium Compositions, Rocket Performance, and Chapman-Jouguet Detonations," NASA TN D-1454 (1962).

TABLE I. - ABSORPTION COEFFICIENT AND ITS TEMPERATURE

COEFFICIENT FOR H_2O AT 1 atm

T_m, K	1000		2000		3000	
λ, μm	$k_0 T_m/T_0{}^a$	H^b	$k_0 T_m/T_0{}^a$	H^b	$k_0 T_m/T_0{}^a$	H^b
6.667	1.13	-0.27	0.807	-0.66	0.525	-1.61
6.557	1.1	-0.78	.562	-0.77	.430	-0.92
2.878	.365	1.32	.353	-0.36	.272	-0.89
2.703	.673	-0.13	.268	-2.45	.150	-2.36
2.685	.566	-1.17	.194	-2.60	.113	-2.15
2.597	.277	-2.77	.161	-0.57	.154	-0.14
2.581	.422	-1.81	.197	-0.79	.177	-0.34
2.532	.358	.41	.230	-1.04	.207	-0.33
2.516	.269	.59	.195	-0.82	.190	-0.08
2.500	.186	.69	.159	-0.50	.161	0.04
2.484	.113	.75	.124	0.0	.132	0.18
1.869	.0844	-0.61	.0593	-0.63	.0480	-0.71
1.810	.0451	.56	.0452	-0.11	.0438	-0.10
1.802	.0369	.89	.0414	-0.06	.0420	0.04
1.794	.0282	1.10	.0366	0.30	.0400	0.25
1.786	.0203	1.26	.0303	0.53	.0360	0.47

[a]This quantity is tabulated, rather than k_0, to facilitate linear inter-polation between columns.

[b]Evaluated at $T_1 = 0.85 T_m$.

TABLE II. - TRANSMISSION FACTORS FOR CURVES

OF FIGURE 5 WITH n = 0.1

| | λ_a, μm = 6.667 | | 6.667 | | 2.703 | |
| | λ_b, μm = 1.786 | | 2.878 | | 2.500 | |
L, cm	$\tau_{L,a}$	$\tau_{L,b}$	$\tau_{L,a}$	$\tau_{L,b}$	$\tau_{L,a}$	$\tau_{L,b}$
4	0.909[c]	0.995[c]	-----	------	-----	------
10	.796	.988[c]	0.796	0.895[c]	-----	------
20	.652	.976[c]	.652	.806	0.864	0.891[c]
50	.399	.941[c]	.399	.610	.710	.761
100	.215	.887[c]	.215	.415	.534	.601

[c]This quantity is $^c\tau_L$. Others are $^m\tau_L$.

Figure Captions

Fig. 1. Assumed temperature profiles characterized by two parameters.

Fig. 2. Parameter F as function of measured or calculated overall transmission factors.

Fig. 3. Values of parameter $f = f(\lambda, H, n, T_m)$.

Fig. 4. Overall transmission factor of an isothermal gas column.

Fig. 5. Error ratios for several wavelength pairs, as function of geometric path length. $T_m = 3000$ K.
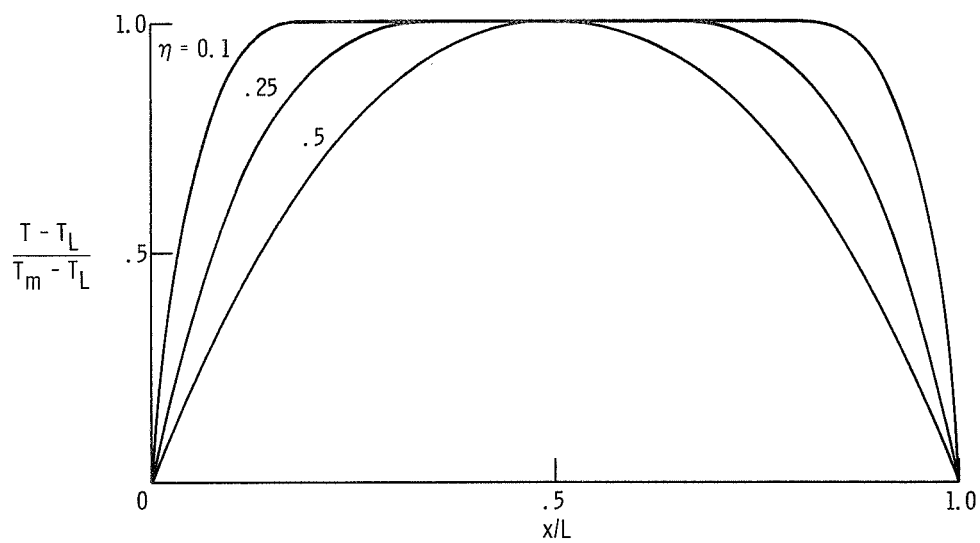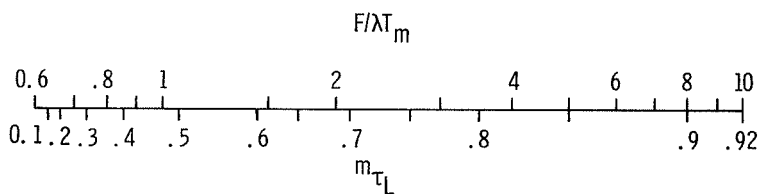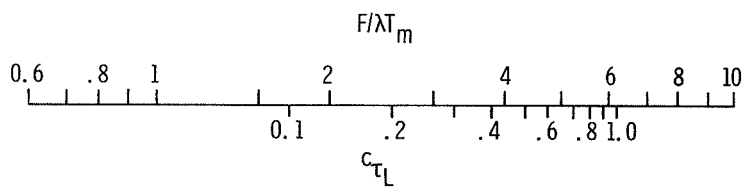
Figure 1

$F/\lambda T_m$

(A) τ_L OBTAINED FROM MEASURED φ_1 AND φ_3.
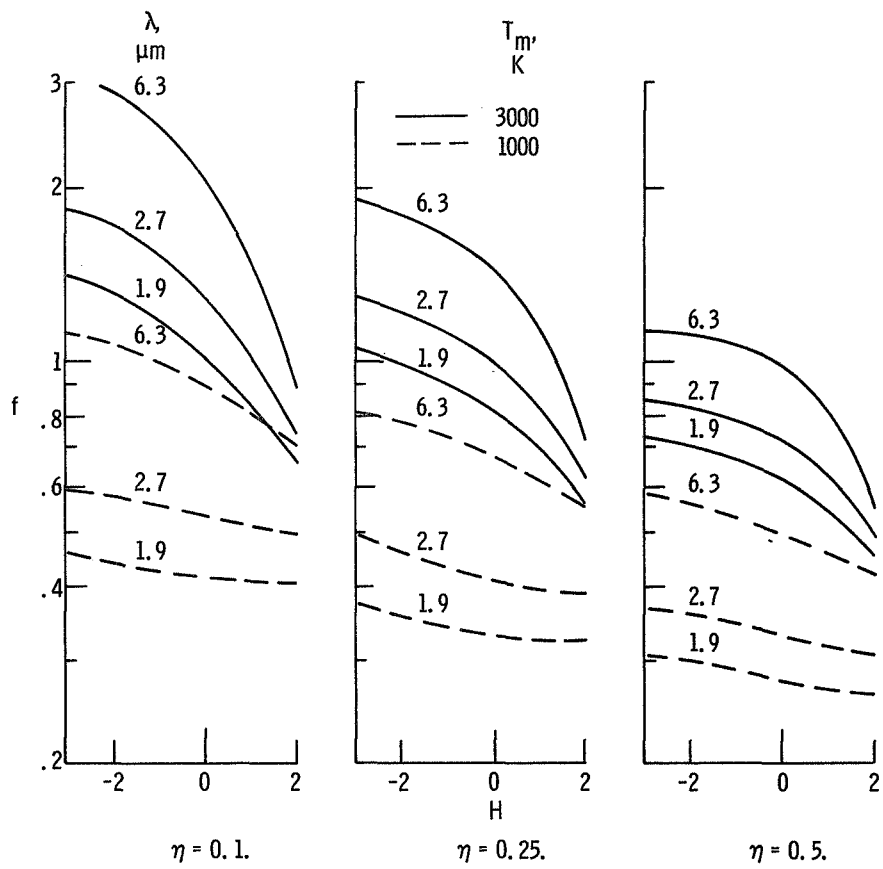
$F/\lambda T_m$

(B) τ_L CALCULATED FROM k AND $T(x)$. (ϵ = 10).

Figure 2

Figure 3

Figure 4

Figure 5